Hadronic Resonance production in ALICE

2017 J. Phys.: Conf. Ser. 878 012003

(http://iopscience.iop.org/1742-6596/878/1/012003)

IOP Conf. Series: Journal of Physics: Conf. Series **878** (2017) 012003 doi:10.1088/1742-6596/878/1/012003

Hadronic Resonance production in ALICE

Christina Markert for the ALICE Collaboration

The University of Texas at Austin, Physics Department, Austin, Texas, USA

E-mail: cmarkert@physics.utexas.edu

Abstract. In heavy ion collisions a fireball of hot and dense matter is created. Short lived hadronic resonances are sensitive to the medium properties, in particular to the temperature, density and system size. Resonance yields and momentum distributions are used to gain insight into the hadronic phase, its expansion velocity and time duration. The multiplicity dependent hadronic resonance production in p-p, p-Pb and Pb-Pb collisions will be discussed within the context of the possible extended hadronic and partonic phase. The experimental results will be compared to EPOS+UrQMD model calculations to discuss the system size dependent interactions of the hadronic medium on various resonances. Small systems such as p-p and p-Pb collisions will be discussed with respect to resonance and strange particle measurements.

1. Introduction

Hadronic resonances interacting throughout the partonic and hadronic phase of heavy ion collisions will leave an imprint from the different stages of the medium on the resonance properties such as mass, width, yield and momentum distribution. Initially we have been motivated to detect invariant mass shifts and width broadenings as chiral symmetry restoration signatures from a transition between the partonic and the hadronic nuclear matter. However, further interaction within the hadronic medium until the kinetic freeze-out will dilute these early signals. This sensitivity to hadronic phase interactions are now used to determine the length and temperature dependence of the hadronic phase which changes the yields and the momentum distribution of the resonances. This can be studied in detail within the centrality dependence of the collisions where the hadronic phase is expected to live the longest in the most central collisions with the highest multiplicity of produced particles. The lifetimes of hadronic phase interactions can be extracted via microscopic model calculations EPOS+UrQMD [1] including the partonic and hadronic phase interactions. The model calculations of resonance yields and momentum distributions are compared to measurements from the ALICE experiment at the LHC which show a general agreement. The suppression of the reconstructed yield of short lived resonances have been observed at RHIC and SPS energies [2] and explained within the UrQMD model [3] by an extended hadronic lifetime. As a further consequence of the hadronic phase interactions stable particle yields may change due to annihilation processes of particles with their antiparticles. This yield changes need to be taken into account when thermal model fits are applied to calculate the chemical freeze-out temperatures. Chemical freeze-out models have successfully described the particle abundance of ground state particles with a minimum set of parameters including the temperature and the baryo-chemical potential [4, 5, 6, 7, 8, 9]. Now hadronic resonance measurements can be used to determine the existence and the lifetime of an extended hadronic phase after chemical freeze-out.

2. Resonance production in Pb-Pb and minimum bias p-p collisions

Short lived resonances are reconstructed via invariant mass through their hadronic decay particles (table 1) which are identified via their masses. This is done in the ALICE detector mainly through the velocity measurement of the Time-Of-Flight (TOF) detector or the energy loss dE/dx in the Time Projection Chamber (TPC) gas where both depend on the momentum measured in the TPC and the Inner Tracking System (ITS). Figure 1 shows the momentum distributions of the $\phi(1020)$ (left) and $K^*(892)^0$ (right) mesons after extracting the invariant mass signal and accounting for detector acceptance and efficiencies. The resonances are measured in different centralities of Pb-Pb collisions selected by the number of charged hadrons ($dN_{ch}/d\eta$) and in p-Pb and p-p collisions [11, 12, 13, 14].

Table 1. The resonances are reconstructed experimentally via their listed decay channels [17].

Resonance	decay channel	branching ratio	lifetime (fm/c)
$\rho(770)^0$	$\pi^+ + \pi^-$	1	1.335
$K^*(892)^0$	$\pi^- + K^+$	0.67	4.16
$\phi(1020)$	$K^+ + K^-$	0.489	46.26

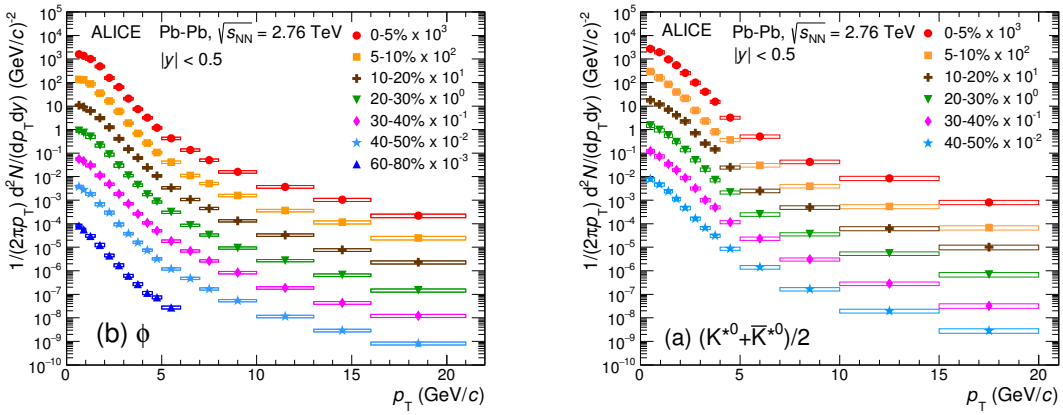

Figure 1. Production of $\phi(1020)$ (left) and $K^*(892)^0$ (right) mesons in p-p and Pb-Pb collisions at 2.76 TeV [11, 12].

The momentum integrated yield normalized to a ground state particle with same or similar quark content ($\phi(1020)$/K, $K^*(892)^0$/K and $\rho(770)^0/\pi$) versus centrality ($(dN_{ch}/d\eta)^{1/3}$ used as a proxy for the system size and radius dependence [10]) are shown in figure 2. The $\phi(1020)$/K is nearly constant while the $K^*(892)^0$/K and $\rho(770)^0/\pi$ are suppresses for larger system size and for more central collisions. Within a statistical model description these particle ratios are mainly determined by the chemical freeze-out temperature T_{ch}, which is the same for different centralities as indicated in figure 3 with T_{ch}= 155 MeV. The predictions of a non-equilibrium model are shown in red triangles. The kinetic freeze-out temperature defined through the end of the elastic interactions of the system decreases with system size (figure 3 blue squares). Due to interactions in the hadronic phase and the smaller cross sections for resonance regeneration the reconstructed resonance yields for shorter lived resonances are expected to be suppressed. The observation of resonance suppression is mainly explained by the lifetime where the $K^*(892)^0$ and $\rho(770)^0$ have the shortest lifetimes (4 and 1.3 fm/c) compared to the $\phi(1020)$ (44 fm/c) (table 1). Since the $\rho(770)^0$ and the $K^*(892)^0$ show the same suppression one would expect that the $\rho(770)^0$ has a larger regeneration cross section from two pions to offset the larger re-scattering due to its three times shorter lifetime compared to the $K^*(892)^0$. EPOS+UrQMD

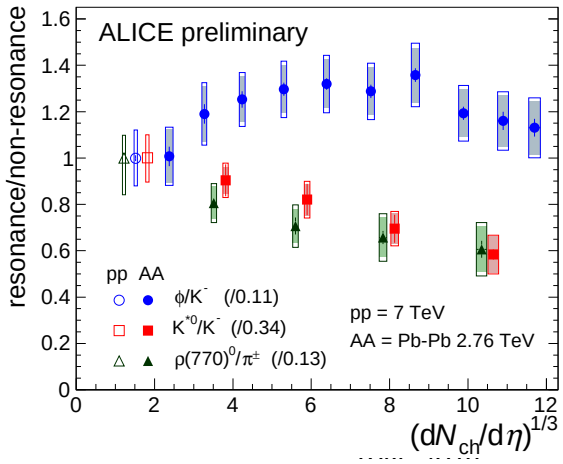

Figure 2. Resonance/non-resonance ratio as a function of charged hadrons for p-p and Pb-Pb collisions

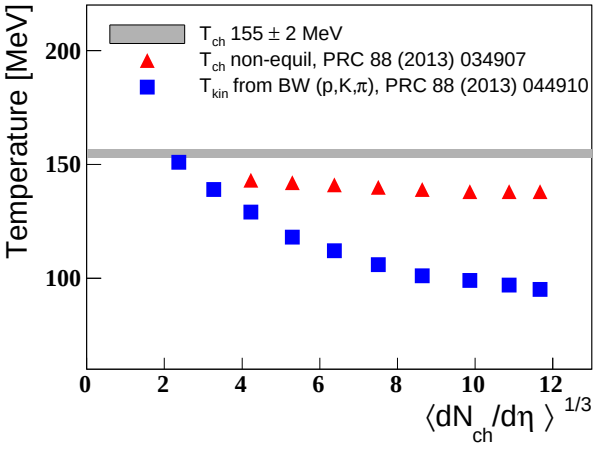

Figure 3. Chemical and kinetic freeze-out temperature as a function of charged hadrons for Pb-Pb collisions.

model predictions are able to describe the $K^*(892)^0$/K and $\rho(770)^0/\pi$ ratio versus $(\mathrm{dN}_{ch}/\mathrm{d}\eta)^{1/3}$ for Pb-Pb collisions at 2.76 TeV. Figure 4 shows the direct comparison of the $\phi(1020)$/K, $K^*(892)^0$/K as a function of charged hadrons [1].

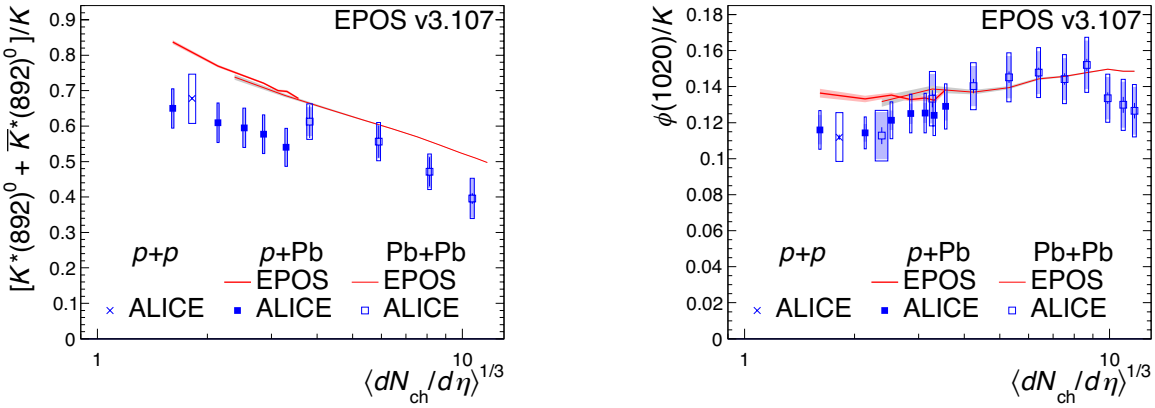

Figure 4. EPOS+UrQMD model calculations for $K^*(892)^0$/K (left) and $\phi(1020)$/K (right) in p-Pb (5.02 TeV) and Pb-Pb (2.76 TeV) collisions (red line) compared to ALICE data for p-p (7 TeV) , p-Pb (5.02 TeV) and Pb-Pb (2.76 TeV) collisions (blue points) [1].

Hadronic phase interactions predominantly occur in the low momentum region and therefore deviation from predicted momentum distributions are expected. The predicted momentum is derived from the shape of the Blast-Wave (BW) model (fit to proton, Kaon and Pion) and the resonance yield from $K^*(892)^0$/K and $\phi(1020)$/K in p-p collisions which are equal to the thermal model predictions for Pb-Pb collisions. The suppression of the $K^*(892)^0$ in the low momentum region for the most central collision 0-20% is visible in Figure 5. While the $\phi(1020)$ does not show any deviation from the predications due to its long lifetime and the reduced interactions of the decay particles in the hadronic medium. Since the BW does not describe the higher momentum $p_T > 2$ GeV/c data very well one would rather focus on the difference of the ratios

$\frac{K^*(892)^0_{data}}{K^*(892)^0_{exp}}$ and $\frac{\phi(1020)_{data}}{\phi(1020)_{exp}}$ (Figure 5 lower panel). EPOS+UrQMD model calculations are able to reproduce the suppression in the low momentum region [1].

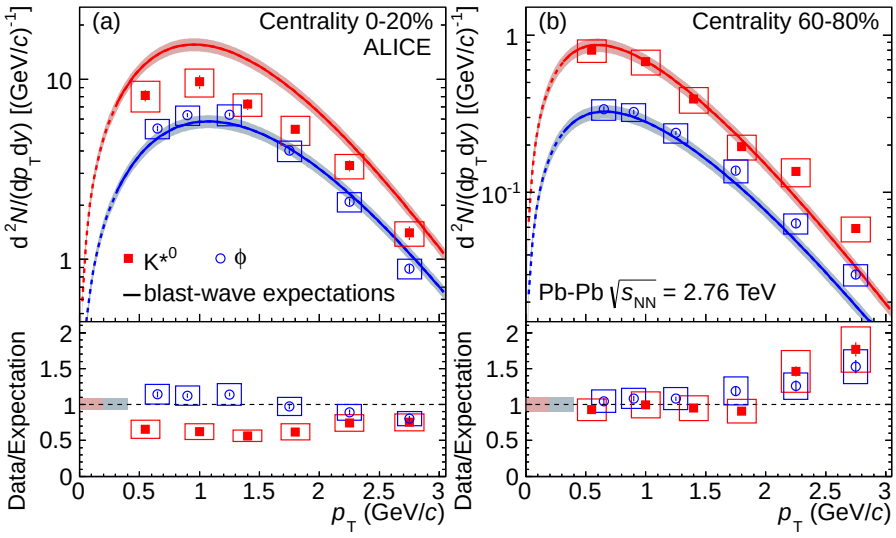

Figure 5. Transverse-momentum distributions of $K^*(892)^0$ and $\phi(1020)$ resonances in Pb-Pb collisions at 2.76 TeV along with expected distributions for central (a) and peripheral (b) collisions. The shapes of the expected distributions are given by Boltzmann-Gibbs blast-wave functions using parameters obtained from fits to $\pi^{\pm}$, $K^{\pm}$, and (anti)proton p_T distributions. The expected distributions are normalized so that their integrals from scaled p-p collisions are equal to the thermal model predictions for Pb-Pb collisions [11]. The lower panel shows the ratio of data divided by the expected value.

3. Influence of hadronic phase on stable particle yields

The statistical model successfully describes the particle yields (short resonances excluded) with a few parameters including the chemical freeze-out temperature (T_{ch}) and the baryochemical potential. The final state particles are a combination of directly produced and feed-down from weak and strong decays. Therefore the yield and the decay properties of the higher mass resonances are important. For example only about 35% of the measured Lambdas are directly produced at T_{ch} = 160 MeV [15]. The particle decay list (decay feed-down list), which are used for the statistical models include some feed-down assumptions from high mass resonances into lower mass resonances such as $\rho(770)^0$, $K^*(892)^0$, $\phi(1020)$, $\Delta(1232)^{++}$, $\Sigma(1385)^{\pm}$, $\Lambda(1520)$ and $\Xi(1530)^0$. These resonances have been measured in p+p and peripheral heavy ion collisions and can be directly compared to the statistical model predictions where the lifetime of the hadronic phase is at its minimum (in more peripheral collisions).

In more central collisions the extended hadronic phase changes the reconstructable resonances due to further interactions of their decay particles within the hadronic medium. This will not change the particles yields of the ground state particles but rather their momentum distribution. However, the annihilation process in the hadronic phase of particle - antiparticles in their ground states will change their yields (e.g. protons, Ξ and Ω). To determine the initial chemical freeze-out temperature (T_{ch}) one needs to account for this effect. Therefore a microscopic model UrQMD was used to study the influence of the hadronic medium on the particle yields after chemical freeze-out [18, 19]. Figure 6 shows the ratio of the final state particle yield normalized to the yield at hadronisation for different densities. The protons and anti-protons show the largest

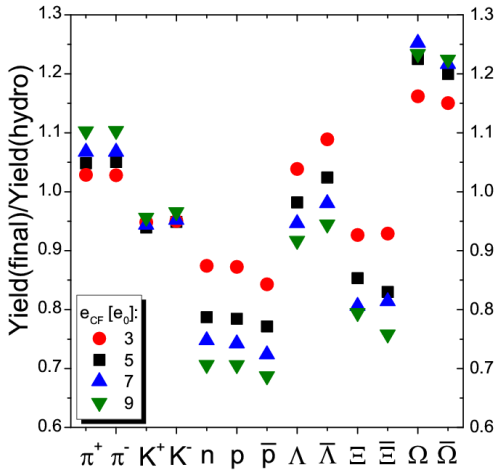

Figure 6. Ratios of particle multiplicities in the final state scaled by the particle multiplicity directly after the hydrodynamic stage for central Pb+Pb collisions at $\sqrt{s_{NN}}$=2.76 TeV. The different symbols denote different transition energy densities [16]

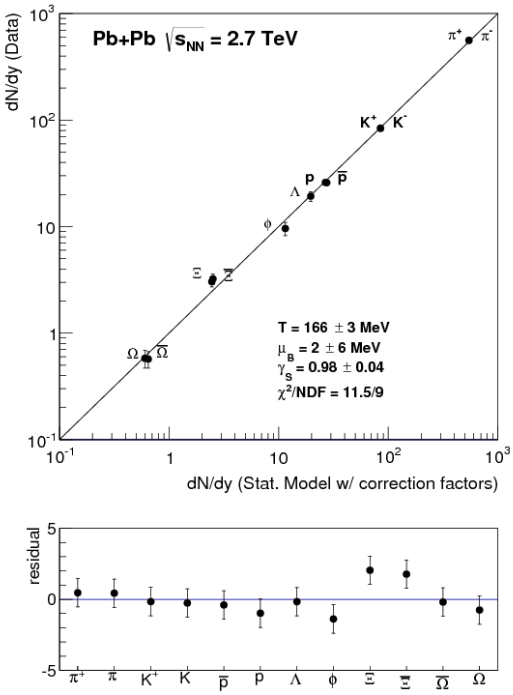

Figure 7. Statistical model fits to preliminary ALICE data for 20% central Pb-Pb collisions at $\sqrt{s_{NN}}$=7 TeV and to the same data but with modification factors from UrQMD applied in the statistical model fits [18].

suppression (absorption), the Ξ's show a smaller suppression and the Ω's show a slight increase. After correcting the hadronic yields for these effects, the thermal model fits are performed. The new temperature increases by 10 MeV and the χ^2/NDF decreases from 26 to 11 as shown in figure 7. This suggests that a systematic error of ΔT=10 MeV is present if hadronic phase interactions are not taken into account. If we understand the interactions of the hadronic phase after hadronisation and chemical freeze-out one can study the impact on correlation signatures. This was done by Steinheimer et. al. [20] who shows that about 50% of the initial fluctuations do not survive the hadronic phase in central heavy ion reactions. It seems to become more difficult to extract partonic phase (Quark Gluon Plasma (QGP)) signals or signals of the phase transition between partonic and hadronic matter when the extended hadronic phase is present. One might look into the more peripheral collisions where the hadronic phase is shorter and the kinetic freeze-out occurs at a higher temperature, or one may find the right momentum range where hadronic phase interactions are at their minimum. On the positive note one can now use resonance measurements to determine the length and expansion conditions of the hadronic phase and estimate its influence on certain observables. In small systems resonances are sensitive to the existence of existence of a possible hadronic phase. This might call into question whether an extended interacting partonic phase such as the QGP is a necessary precursor of the extended hadronic phase with high particle multiplicity.

4. Medium in small systems (p-Pb and p-p collisions)

Recent event multiplicity dependent $K^*(892)^0$ and $\phi(1020)$ measurements in small systems such as p-p and p-Pb are shown in Figure 8. The suppression of $K^*(892)^0$ follows the same trend with increasing multiplicity. The $\phi(1020)$ p-Pb is in agreement with the Pb-Pb results with no suppression due to its large lifetime. It seems that the suppression of the $K^*(892)^0$ is larger in small systems than in Pb-Pb collisions with same track multiplicity. The comparison to EPOS+UrQMD calculations in Figure 4 shows a good description of the trend with a smooth transition from small to large systems. EPOS includes in its description a QGP for the core and and single pQCD processes in the corona area. With this description a QGP is implemented by design. In this case the p-Pb collisions show the same dependence on the particle multiplicity as in Pb-Pb collisions. However, the data show a slightly larger suppression for the $K^*(892)^0$ in p-Pb than predicted by the model. And the p-p collisions show an even larger suppression (Figure 8). One can ask if the number of produced charged particles is the correct scaling variable or if the density which is larger in the small volumes of the collision systems plays a role in the scaling as well. If the suppression of the $K^*(892)^0$ resonance is caused by an extended hadronic phase then the EPOS+UrQMD model calculation estimates a lifetime of about 2 fm/c for the 0-5% highest multiplicity for the p-Pb collisions.

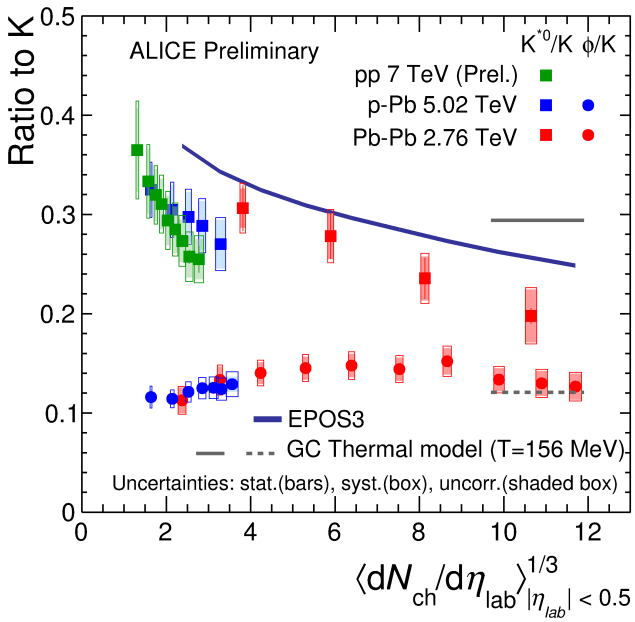

Figure 8. Resonance to stable particle ratio in p-p collisions at 7 TeV, p-Pb collisions at 5.02 TeV and Pb-Pb at 2.76 TeV for different multiplicity event classes comparison with other systems. The statistical uncertainties are shown as bars, systematic errors in boxes, and uncorrelated systematic errors in shaded boxes.

Differences in the dynamical evolution of the small systems is described by the transverse expansion velocity β_T, which drives the mean transverse momentum $\langle p_T \rangle$ and the kinetic freeze-out temperature, which is defined by the end of the elastic interactions. Figure 9 shows a steeper increase of the $\langle p_T \rangle$ for the smaller systems with increasing number of charged particles. Both resonances with similar masses as the proton, $\phi(1020)$ (80 MeV/c^2 larger) and $K^*(892)^0$ (40 MeV/c^2 smaller), show a larger $\langle p_T \rangle$ than the protons in p-p and p-Pb collisions. In Pb-Pb collisions the $K^*(892)^0$ follows the trend of the protons while the $\phi(1020)$ shows a lager $\langle p_T \rangle$ in peripheral collisions with a small increase with increasing centrality until it is in agreement with the values for protons in mid-central collisions. The number of charged hadrons in 0-5% p-Pb is the same as in 60-80% Pb-Pb collisions. However, the momentum spectra show a different expansion dynamics in this collision system. How much of the $\langle p_T \rangle$ change might be driven by a possible QGP phase in 0-5% p-Pb collisions is not clear at this moment.

Another observable in small systems is the strangeness production which shows increasing

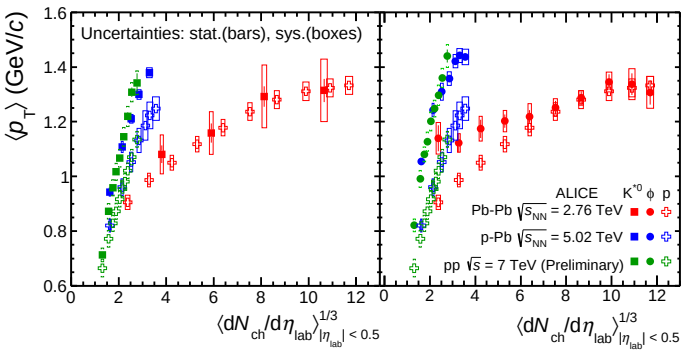

Figure 9. Mean transverse momentum $\langle p_{\mathrm{T}} \rangle$ of protons for p-p, p-Pb and Pb-Pb collisions compared to $K^*(892)^0$ (left) and $\phi(1020)$ (right).

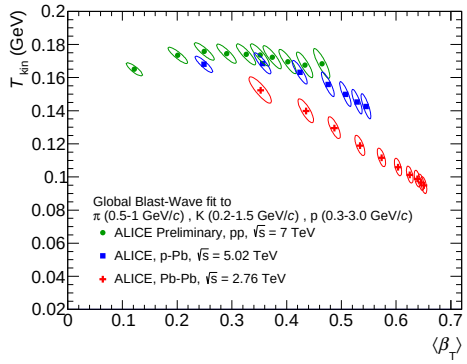

Figure 10. Expansion parameter transverse velocity β_{T} and kinetic freeze-out temperature T_{kin} from a Blast-Wave fit to π, K and p spectra measured in Pb-Pb collisions at 5.02 TeV.

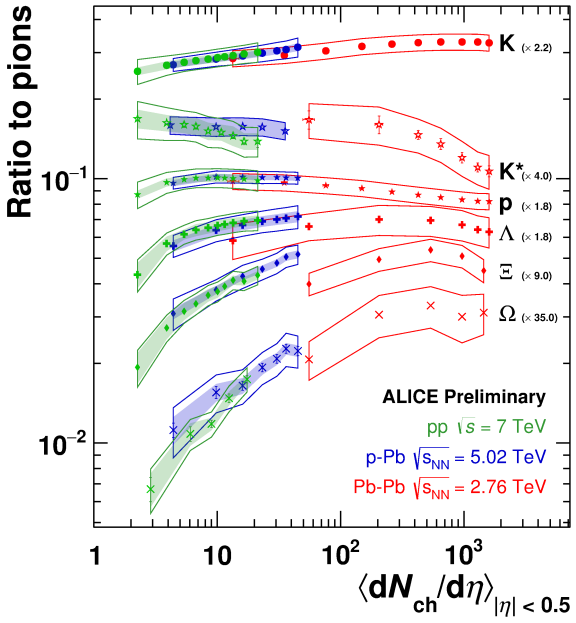

Figure 11. Particle yield ratio to pions of various identified particle species as a function of $\langle dN_{ch}/d\eta \rangle$ (measured at $|\eta| < 0.5$) in pp at 7 TeV, compared to pPb at 5.02 TeV and PbPb at 2.76 TeV. The hollow error band indicates the total systematic uncertainties, the shaded ones are the systematic uncertainties that are independent of multiplicity (latter only shown for pp and pPb).

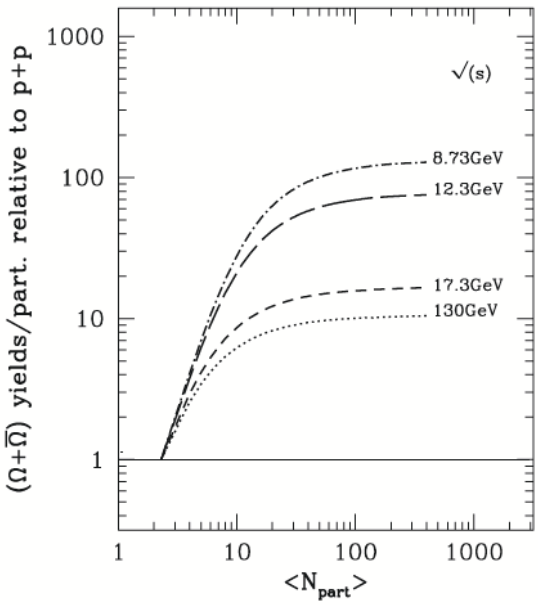

Figure 12. Centrality dependence of relative enhancement $(\Omega + \bar{\Omega})$ Yields/participant in central Pb-Pb to p-p reactions at different collisions energies.

strangeness/non-strangeness particle ratio. The strangeness production was suggested as one of the initial signatures for the QGP [21]. The increase of strangeness production as a function of centrality (charged particle multiplicity) with respect to the production in p-p collisions is shown in figure 11. This trend can be exlpained mainly driven by the strangeness suppression in p-p collisions due to a canonical description (small system size). The increase in heavy ion reactions is rather a vanishing of the strangeness suppression in small systems. This volume effect was calculated by K. Redlich for RHIC energies [22] (figure 12). Since the increase is rather a volume effect, the "real" strangeness enhancement is an enhancement in addition to the volume effect. The "real" strangeness enhancement has never been confirmed in heavy ion reactions within its statistical and systematical uncertainties. It might be also due to the difficulty of defining the turning point (volume and particle multiplicity) where the canonical system fully transfers into a grand canonical system.

The new strangeness production results in small systems from ALICE in p-p and p-Pb collisions with increasing number of produced hadrons show the same trend of the volume dependence. However, the volume effect of a canonical system also needs to be taken into account here. For sure the increase of strangeness production is an indication of the interactions of the extended hadronic phase. Whether this is driven by a extended partonic QGP phase cannot be answered at this point. Further investigation of the volume effect should help us to have a new look at this data to extract any possible signature of a QGP.

Acknowledgments

I would like to thank the organizer for inviting me to this very nice place, which stimulated very fruitful discussions in our field. The friendliness and open atmosphere allowed a deeper and critical discussion. I really enjoyed it very much and I was happy to be surrounded by this energetic and friendly group of scientists. I also would like to thank the ALICE collaboration for supporting my presentation.

References

[1] A.G. Knospe, C. Markert, K. Werner, J. Steinheimer, M. Bleicher, Phys.Rev. **C93** (2016) no.1, 014911.
[2] B.I. Abelev et al., (STAR Collaboration), Phys. Rev. Lett. **97**, 132301 (2006)
[3] M. Bleicher *et al.*, Phys. Lett. **B530**, 81 (2002);
M. Bleicher, Nucl. Phys. **A715**, 85 (2003).
[4] J. Cleymans, K. Redlich, Phys. Rev. Lett. **81** (1998) 52845286.
[5] J. Cleymans, H. Oeschler, K. Redlich, S. Wheaton, Phys.Rev. **C73** (2006) 034905.
[6] F. Becattini et al, JPG 025002 (2011)
[7] R. Rafelski, Letessier, Phys. Rev. **C83**, 054909 (2011)
[8] M. Petran, J. Letessier, V. Petracek, J. Rafelski, Phys.Rev. **C88** (3) (2013) 034907.
[9] P. Braun-Munzinger, K. Redlich, J. Stachel arXiv:nucl-th/0304013.
[10] K. Aamodt et al. Phys.Lett. **B696** (2011) 328-337
[11] B. Bezverkhny Abelev *et al.* (ALICE collaboration), Phys. Rev. **C91** 2, (2015) 024609.
[12] J. Adam et al., arXiv:1702.00555 [nucl-ex]
[13] J. Adam et al., Eur. Phys. J. **C76** (2016) no.5, 245.
[14] B. Abelev et al., Eur. Phys. J. **C72** (2012) 2183.
[15] J. Letessier, J. Rafelski, Cambridge Monographs on Particle Physics and Cosmology page 31 (2002).
[16] J. Steinheimer, J. Aichelin, M. Bleicher, Phys. Rev. Lett. **110** (2013) no.4, 042501.
[17] K. A. Olive *et al.* (Particle Data Group), Chin. Phys. **C38**, 090001 (2014)
[18] F. Becattini, M. Bleicher, T. Kollegger, T. Schuster, J. Steinheimer, R. Stock, Phys. Rev. Lett. **111** (2013) 082302.
[19] F. Becattini, E. Grossi, M Bleicher, J. Steinheimer, R. Stock, Phys. Rev. C90 (2014) no.5, 054907.
[20] J. Steinheimer, V. Vovchenko, J. Aichelin, M. Bleicher, H. Stöcker, Aug 12, 2016, arXiv:1608.03737.
[21] J. Rafelski, B. Muller, Phys. Rev. Lett. 48 (1982) 1066.
[22] A. Tounsi, K. Redlich, J.Phys. G28 (2002) 2095-2102.